
Planetary Nebulae Principles & Paradigms: Binaries, Accretion, Magnetic Fields

Eric G. Blackman and Jason T. Nordhaus

Department of Physics and Astronomy, University of Rochester, Rochester, NY,
14627, USA, blackman@pas.rochester.edu

Summary. Observations suggest that many, if not all, post AGB systems evolve through an aspherical outflow phase. Such outflows require a sufficient engine rotational energy which binaries can provide. Via common envelope evolution, binaries can directly eject equatorial outflows or produce poloidal outflows from magnetized accretion disks around the primary or secondary. We discuss how accretion driven magnetohydrodynamic outflow models all make similar predictions for the outflow power and speed and we distinguish between the launch vs. propagation regimes of such outflows. We suggest that the high velocity bipolar outflows observed in planetary nebulae (PNe) and the lower velocity but higher power bipolar outflows observed in pre-PNe (pPNe) are kinematically consistent with time dependent accretion onto a white dwarf (WD) within a depleting envelope. Since the WD primary core is always present in all post-AGB systems, accretion onto this core is potentially common. Previous work has focused on core accretion from sub-stellar companions, but low mass stellar companions may be more important, and further work is needed.

Key words: stars: AGB and post-AGB; (stars:) binaries: general; accretion, accretion disks; magnetic fields; stars: winds, outflows

1 Introduction: Kinematics of pPNe and PNe

Understanding the origin of asymmetric outflows in PNe and pPNe requires feedback between observers, specific object modelers, and paradigm-seeking, order of magnitude theorists. Here we behave as the latter.

Generally, pPNe exhibit a combination of a fast bipolar outflow embedded within a slow spherically symmetric wind from the AGB star [6]. Presently, the data do not rule out all pPNe having gone through a strongly asymmetric outflow and all PNe having gone through an asymmetric pNE phase. The symmetry of PNe would then correlate with age and the evolution from the pPNe to PNe could reflect a time evolution of the same physical mechanism that produces asymmetry on small scales but leads to a nearly spherical structure on large scale as supersonic motions damp. While AGB stars produce spherically symmetric outflows, pPNe asymmetry arises within ≤ 100 yr [6, 24].

For pPNe [6], each fast wind has a typical age $\Delta t \sim 10^2 - 10^3$ yr, speed ~ 50 km/s, mass $M_f \sim 0.5M_\odot$, outflow rate, $\dot{M}_f \sim 5 \times 10^{-4}M_\odot/\text{yr}$, momentum $\Pi \sim 5 \times 10^{39}$ g.cm/s, and mechanical luminosity $L_{m,f} \geq 8 \times 10^{35}$ erg/s (can be as high as 10^{37} erg/s). The slow pPNe wind has an age $\Delta t \sim 6 \times 10^3$ yr, a speed $v_w \sim 20$ km/s a mass $M_s \sim 0.5M_\odot$, outflow rate, $\dot{M}_s \sim 10^{-4}M_\odot/\text{yr}$, momentum $\Pi_s \sim 2 \times 10^{39}$ g cm/s, and mechanical luminosity $L_{m,s} \sim 10^{34}$ erg/s.

For PNe observations suggest e.g. [2] an age $\Delta t \sim 10^4$ yr a slow wind of speed $v_s \sim 30$ km/s of mass $M_s \sim 0.1M_\odot$, outflow rate, $\dot{M}_s \sim 10^{-5}M_\odot/\text{yr}$, momentum $\Pi_s \sim 6 \times 10^{38}$ g cm/s, and mechanical luminosity $L_{m,s} \sim 3 \times 10^{33}$ erg/s. PNe have fast winds of speed $v_f \sim 2000$ km/s, mass $M_f \sim 10^{-4}M_\odot$, outflow rate, $\dot{M}_f \sim 10^{-8}M_\odot/\text{yr}$, momentum $\Pi_f \sim 4 \times 10^{37}$ g cm/s, and mechanical luminosity $L_{m,f} \sim 1.3 \times 10^{34}$ erg/s.

The pPNe phase demands the most power. The linear momenta of fast bipolar pPNe outflows seems too large for radiation driving [6]. This motivates the need to tap rotational energy which binaries can provide. The high fraction of binaries attributed to p/PNe has led to speculation that all asymmetric PNe and pPNe involve binaries [16, 22].

How is the rotational energy and angular momentum converted into outflows? Differential rotation supplied by binaries can amplify magnetic fields which can in turn produce accretion powered bipolar jets. Accretion powered, magnetically mediated jets, are seemingly ubiquitous in astrophysics and can accommodate the high momentum pPNe demands [5].

2 Which Binary Accretion Scenario?

In a common envelope (CE) [13] the companion drags on the envelope of the primary, transferring angular momentum and kinetic energy. Provided that the envelope cooling time scale exceeds the energy supply time from the in-spiraling companion, a converted fraction $\alpha \geq 0.1$ of its loss in gravitational energy can spin up the envelope and unbind it. For a fixed envelope mass, a lower mass companion must fall deeper to unbind the envelope. Fig. 1 [17] shows aspects of CE for low mass companions in an AGB envelope. When the Roche radius is reached by the in-spiraling companion, accretion can occur.

Ref. [20] discusses the secondaries for which accretion disks will form around the primary core. Brown dwarf (BD) ($0.003M_\odot < M_{crit} \sim 0.07M_\odot$) radii increase with decreasing mass unlike their Roche radii which decrease with decreasing mass. Such objects will unstably lose mass. Since the circularization radius lies outside of the primary's core, a disk can form within a few orbit times. This contrasts the $M > M_{crit}$ case for which the stellar radius decreases with decreasing mass and more strongly so than the Roche radius. Supercritical companions present a circularization radius *within* the primary's core. Material leaving the secondary would then initially spiral swiftly into the primary rather than orbit quasi-stably.

Ref. [20] focuses on BDs ($0.003M_\odot < M_2 < M_{crit}$), but accretion from low mass stars and planets warrant further study: Fig.1 (left) shows that for low values of the (uncertain) drag parameter α , some low mass stars could tidally shred into a disk before reaching the radius where they unbind the envelope and subsequent in-spiraling is potentially slowed. Fig. 1 also shows that planets will shred into a

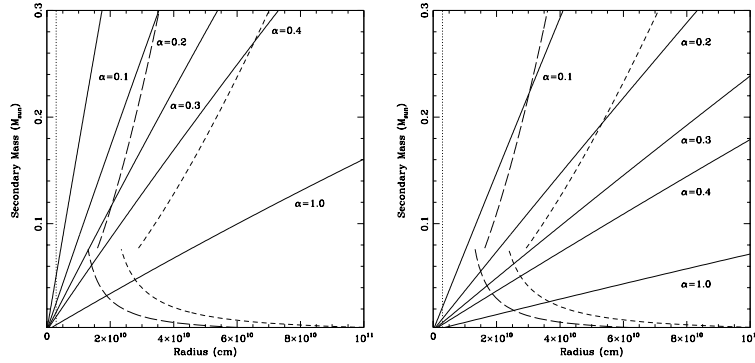


Fig. 1. From [17]: For a $3M_{\odot}$ young AGB star (left) and inter-pulse AGB star (right), the solid lines show the radius where a companion must in-spiral to unbind the envelope for different values of the drag parameter α . The dash-dotted line shows the core-envelope boundary. The long-dashed line marks the tidal shredding radius and the short dashed line is where the companion first fills its Roche lobe.

disk upon inspiral and for large α in the inter-pulse AGB, even large planets might unbind the envelope. Generalizations must incorporate the fact that the companion size can be of order the tidal shredding or Roche lobe radius, and the structural evolution of the primary as the secondary in-spirals. The latter is important for radii both exterior and interior to the companion: How fast do further inspiral and angular momentum transfer subsequently occur once the outer envelope is ejected?

If a stellar companion unbinds the envelope at a radius with Roche lobe overflow but without tidal shredding, sustained accretion requires the binary to lose angular momentum. As the secondary fills its Roche lobe, it will drag on any residual inner envelope material. This could transfer the needed angular momentum, but too much drag could prevent the companion from forming a quasi-stable Keplerian disk. Material that initially leaves the companion for the primary also carries magnetic fields and thus will magnetically link the primary and secondary. Even though the circularization radius for $M_2 > M_{crit}$ is inside the core, the in-spiraling material still incurs differential rotation. Magnetic fields can then be amplified and can also release angular momentum.

Much of the initial accreted energy in the $M_2 > M_{crit}$ case would be released upon material impact to stellar surface. This could produce dwarf novae type bursts shrouded by the stellar envelope. However, if the right range of mass and angular momentum are transferred in this initial accretion phase to (1) drop M_2 below M_{crit} , (2) keep M_2 filling its Roche lobe, and (3) leave enough angular momentum to form a Keplerian disk, then accretion could proceed as for the initial $M_2 < M_{crit}$ case of Ref.[20]. Ref. [12] suggests a $\sim O(100)$ year delay in the time scale between ejection of circumbinary dust tori and presence of jets in pPNe. If the companion initially has $M_2 > M_{crit}$, the fraction of the envelope ejected as it spirals in might become the dust torus, and the delay before the jet could be the time it takes for the companion to lose enough mass to move the circularization radius outside the core.

The role of low mass stellar and planetary companions is important because although $\sim 16\%$ of nearby ($< 50\text{pc}$) sun-like (late F to early K) stars have companions more massive than Jupiter at $< 3\text{AU}$, 11% are stars, 5% are planets, and 0% are BDs [11]. If this $\sim 16\%$ were crudely taken as the fraction of binary induced, and thus asymmetric p/PNe, this is within a factor of 2 of estimates of the total fraction of low mass stars incurring any PNe [22].

It is also possible for accretion disks to form around the secondary [23, 14, 21]. The accretion rate inferred from the Bondi wind accretion formulae is

$$\frac{\dot{M}}{\dot{M}_s} = \left(\frac{M_2}{M_1}\right)^2 \frac{(v/v_s)^4}{[1 + (v/v_s)^2]^{3/2}}, \quad (1)$$

where v is the orbital speed of the secondary and v_w is the slow wind speed from the primary. In general, for $M_2 < M_1$, reasonable parameters provide an accretion rate compatible with the luminosities required at the PNe stage if the companion is a main sequence star. However, the outflow velocities of the fast wind in PNe would require a WD companion, as seen in the next section. Complementarily, the luminosities of the fast wind pPNe outflows would also require a WD companion.

3 Accretion Disk Outflows in pPNe and PNe:

Accretion disk outflows have a mechanical luminosity of order [5]

$$L_m \sim \frac{GM_*\dot{M}_a\epsilon}{2R_i} = 4.5 \times 10^{36} \epsilon_{-1} \frac{M_*\dot{M}_{-4}}{R_{i,10}}, \quad (2)$$

where ϵ is the dimensionless efficiency of conversion from accretion to outflow, R_i is the inner disk radius, \dot{M}_a is the accretion rate, G is Newton's constant, and M_* is the central stellar mass. In the last term $R_{i,10} \equiv R_i/10^{10}\text{cm}$, $\epsilon_{-1} \equiv \epsilon/0.1$ and $\dot{M}_{a,-4} = \dot{M}_a/10^{-4}M_\odot/\text{yr}$. For an MHD outflow, Eq. (2) equals the Poynting flux at the launch surface.

For propagation into a region of negligible inertia, the asymptotic outflow speed is $\sim \Omega r_A$ [19] where Ω is the angular speed of field anchor point and r_A is the radius where the poloidal outflow speed equals the Alfvén speed. This product is typically of order 1-3 times the escape speed of the inner most radius of the disk and is thus at least

$$v_{out} \sim v_{esc} = 1600 \left(\frac{M_*}{R_{*,10}}\right)^{1/2} \text{ km/s}. \quad (3)$$

Time dependent accretion outflows described with Eqs. (2) and (3) are consistent with the high pPNe outflow mechanical luminosity and the fast PNe wind speed of Sec. 1 when M_*/R_* corresponds to a WD (for accretion onto primary $M_* = M_1$, or secondary $M_* = M_2$). The outflow speed from (3) does not depend explicitly on \dot{M}_a (only implicitly and weakly via R_i which can exceed the stellar radius for a strong field) and is thus largely time independent. However, this speed depends on the inertia of material blocking the outflow. Conservation of momentum gives

$$v_{obs} = \frac{M_f v_f}{f_\Omega M_{env} + M_f} \sim 80\text{km/s}, \quad (4)$$

where $M_f/M_\odot = 3.3 \times 10^{-4} \epsilon_{-1} \dot{M}_{a0,-3} \int_1^{1000} \tau^{-5/4} d\tau$ is the mass in one of the fast collimated outflows, M_{env} is the envelope mass, $f_\Omega \sim 0.2$ is the solid angle fraction intercepted by the collimated outflow, and $\tau \equiv t/1yr$ is used to incorporate $\dot{M}_a \propto t^{-5/4}$ of Ref. [20]. The numbers have been scaled to the pPNe case so that here $M_{env} \gg M_f$ and for an envelope of mass $2M_\odot$, giving the intercepted mass of $0.2M_\odot$ for $f_\Omega = 0.2$. Eq. (4) then implies $v_{obs} = 40\text{km/s}$, within the range observed [2].

Eq. (4) represents the observed speed of the fast when blocked and loaded by the envelope. By the end of the pPNe phase, the envelope is quite extended, reducing the optical depth and revealing material moving at the “free streaming” fast wind speed. Assuming a dust-to-gas mass ratio of 1/100 and micron sized grains of density of 2g/cm^3 , the optical depth from dust is

$$\tau_d \sim 2.5 \times 10^{-3} \left(\frac{n_d}{2.5 \times 10^{-13} \text{cm}^{-3}} \right) \left(\frac{\sigma_d}{10^{-8} \text{cm}^2} \right) \left(\frac{R}{10^{18} \text{cm}} \right), \quad (5)$$

scaled for PNe. For pPNe, the density increases by a factor $\geq 10^4$ and R is down by a factor of 10, so $\tau_d \geq 2.5$, optically thick. The different optical depths of pPNe and PNe can thus explain why observed PNe fast winds can have $v_f > 1600\text{km/s}$, whilst those of pPNe have $v_f < 100\text{km/s}$.

Keeping in mind our discussion of low mass stellar companions in Sec 2, note that Ref. [20] considers a companion of mass $M_2 \sim 0.03M_\odot < M_{crit}$ and a Shakura-Sunyaev viscosity parameter $\alpha_{ss} \sim 0.01$, for which the accretion rate then decays as $\dot{M}_a \sim 1.6 \times 10^{-3} t^{-5/4} M_\odot/\text{yr}$. Using this in (2) with $\epsilon = 0.1$ for $t = 100$ yr with $R_i = 2 \times 10^9 \text{cm}$ and $M_1 = 0.6M_\odot$ gives $L_{m,f} \sim 4.3 \times 10^{39} (t/1\text{yr})^{-5/4}$. This provides the needed power demands of Sec. 1 for pPNe after 1000 yr and for PNe after 10^4 yr.

Because the surface density evolves, the gas opacity evolves from Thomson to Kramer’s after ~ 100 yr [20], and the height to radius ratio decreases substantially as the disk cools. A fixed $\alpha_{ss} \sim 0.01$ is self-consistent with the time evolving accretion and power above.

4 Launch versus Propagation Regions for MHD Outflows

We refer to the “launch” region [3] of MHD outflows as the region where the magnetic force and energy dominates the flow and thermal energy. This extends to a height typically no greater than $z_c \sim 10 - 50R_i$, where R_i is the innermost radial scale of the engine (e.g. the inner radius of an accretion disk). In the launch region the bulk flow is accelerating but is sub-Alfénic until reaching z_c . The “propagation” region describes $z > z_c$ where the poloidal flow speed exceeds the Alfén speed, eventually approaching its asymptotic speed. Presently, only the propagation region is observationally spatially resolved. With this distinction, we describe 3 classes of MHD outflow related work.

Launch to Propagation: e.g. [15, 10, 1]; Here the magnetic field is imposed to be ordered on a scale at least as large as the anchoring rotator. The base of the rotator is typically a boundary condition. Calculations address how material is accelerated by the combination of centrifugal flinging of material along quasi-rigid field lines and/or a vertical gradient in the magnetic pressure. Both a poloidal and toroidal field component at the base are required. The flow can be collimated and supersonic

by hoop stresses before upon reaching the propagation region provided that there is an ambient pressure to collimate the magnetic field. Simulations can cover from the base of the launch region to a scale typically ≤ 100 times the engine scale.

Asymptotic Propagation: e.g. [9, 7]; Here a collimated jet is injected on small scales, and the subsequent propagation and shaping by the ambient medium of specified magnetic and thermal properties is studied. The jet and ambient medium parameters are varied to assess what conditions can produce the observed asymptotic, morphologies. These simulations do not address the magnetic field origin or acceleration mechanism.

Field Origin to Launch: e.g.[5, 18]; The previous two categories do not address where the dynamically important large scale fields comes from in the first place. Accretion of flux may be difficult in a turbulent disk, but these large scale fields can plausibly be produced by a combination of a flow dominated helical dynamo inside of the rotator, followed by magnetic buoyancy, and a magnetically dominated helical dynamo relaxation in the corona [4]. The latter opens up structures to the large scales needed to drive jets, much as solar coronal loops open to create solar coronal holes. This category of work focuses on the field origin, with kinematic estimates of the subsequent launch, but not the dynamical launch itself.

It is a frontier to couple the above categories, and each has limitations when separated from the other two. For example, a self-consistently grown strong field dynamically mediating the launch need not necessarily imply a strong magnetic influence in the propagation region: If the launch region produces a super-magnetosonic collimated outflow, then even subsequent ballistic propagation into the propagation region would still emerge as collimated. In addition, a super-magnetosonic outflow could become turbulent and the turbulence can amplify small scale magnetic energy to $> 10\%$ of equipartition with this turbulence. This can be a substantial fraction of the initial bulk flow energy and such a field would be responding to the flow, not the reverse.

To summarize: the physics of the launch region ($< 1AU$) involves: (1) Origin of large scale magnetic fields, field buoyancy to coroneae, field relaxation into larger coronal structures, (2) physics of centrifugal + magnetic acceleration of material from small to super-Alfvénic speeds, or Poynting flux driven bursts of acceleration, (3) criteria for steady or bursty jets, and (4) assessment of the extent of Poynting flux domination.

The physics of the propagation region ($>> 1AU$ observationally resolved) involves such issues as: (1) Propagation, instability formation, and sustenance of collimation in as a function of internal vs. external density and strength of magnetic fields, (2) bow shocks, cocoon physics, particle acceleration, (3) effect of cooling on morphology, and (4) interaction with ambient media.

5 Toward Connections between Theory and Observation

Spatially resolving the launch region and measuring the magnetic field strength and geometry therein would be the gold standard for directly evaluating the role of magnetic fields in producing asymmetric p/PNe. Measurements of fields in the propagation region provide primarily indirect evidence, though the detection of relatively strong fields there is particularly significant [24].

Whether binaries supply needed rotational energy to amplify jet-mediating fields in accretion disks is a fundamental question. The basic wind kinematics are roughly consistent with accretion onto a WD, suggesting the importance of accretion onto the primary.

Coupling accretion disk physics to large scale magnetic field production, to jet launch, and jet propagation in a unified theory is work in progress that spans several subfields of theoretical astrophysics, let alone the specific application to p/PNe. However some predictions/trends can be studied: (1) It should be possible to evaluate the kinematic constraints/predictions of Sec 3 in more detail and compare the distribution of inferred fast outflow speeds to what would be expected from known binary statistics of low mass main sequence stars. This would serve to help determine the commonality of accretion onto the companion vs. the primary. (2) CE models would predict mostly Oxygen rich rather than Carbon rich post AGB systems because typically, the companion ejects the envelope on time scales of order years, right from the beginning of the AGB phase when the envelope expands, so the AGB star would not have had a chance to reach the Carbon dredge up. (3) Crystalline dust in post-AGB systems can be produced if a binary induced spiral shock anneals silicates [8]. Is this universal? (4) CE evolution would predict equatorial outflows from companion inspiral that precedes any accretion driven poloidal jet. A delay is observed [12] but more work is needed to predict the delay time scale. (5) Are the geometry and composition of dust tori around post-AGB objects consistent with the influence of a binary? (6) Are fast outflows contaminated by material that could represent accretion disk residue of shredded low mass companions? (7) Are time scales of observed outflow precession consistent with the gravitational influence of a binary on a disk? (8) Can double peaked line profiles be detected to identify accretion disks within the launch region? (9) Can shrouded novae outbursts from a $M_2 > M_{crit}$ companion feeding the primary be detected in X-rays? (10) Improved statistics on the fraction of bipolar pPNe, the fraction of suitable precursor binaries for CEE, and the fraction of stars which evolve to be pPNe will constrain theories and assess whether all PNe incur asymmetry.

References

1. J.M. Anderson, Z.Y. Li, R. Krasnopolsky, & R.D. Blandford, 2006, ApJ, **653**, L33 (2006)
2. B. Balick, & A. Frank, ARAA, **40**, 439 (2002)
3. E.G. Blackman, Astrphys. Sp. Sci., **307**, 7, (2007)
4. E.G. Blackman, arXiv:0707.3191, New. J. Phys, in press (2007)
5. E.G. Blackman, A., Frank, & C. Welch, ApJ, **546**, 288 (2001)
6. V. Bujarrabal, V., A. Castro-Carrizo, J. Alcolea, & C. Sánchez Contreras, A&A, **377**, 868 (2001)
7. T.J. Dennis A.J.Cunningham, A. Frank, B. Balick, E.G. Blackman, & S. Mitran arXiv:0707.1641 submitted to ApJ (2007)
8. R.G. Edgar, E.G. Blackman, J.T. Nordhaus, A. Frank, in preparation (2007)
9. G. García-Segura, ApJ, **489**, L189 (1997)
10. G. García-Segura, J.A. López, & J. Franco, ApJ, **618**, 919 (2005)
11. D. Grether, & C.H. Lineweaver, ApJ, **640**, 1051 (2006)
12. P.J. Huggins, ApJ, **663**, 342 (2007)

13. I.J. Iben, & M. Livio, *PASP*, **105**, 1373 (1993)
14. N. Mastrodemos, & M. Morris 1998, *ApJ*, **497**, 303 (1998)
15. S. Matt, A. Frank & E.G. Blackman, *ApJ*, **647**, L45 (2006)
16. M. Moe & O. De Marco, *ApJ*, **650**, 916 (2006)
17. J. Nordhaus & E.G. Blackman, *MNRAS*, **370**, (2006)
18. J. Nordhaus, E.G. Blackman, & A. Frank, *MNRAS*, **376**, 599 (2007)
19. R.E. Pudritz, Les Houches Summer School, **78**, 187 (2004)
20. M. Reyes-Ruiz, & J.A. López, *ApJ*, **524**, 952 (1999)
21. N. Soker, *AJ*, **129**, 947 (2005)
22. N. Soker, *ApJ*, **645**, L57 (2006)
23. N. Soker, & M. Livio, *ApJ*, **421**, 219 (2004)
24. W.H.T. Vlemmings, P.J.Diamond, & H. Imai, *Nature*, 440, **58** (2006)